Received: 16 January 2023 | Revised: 20 February 2023 | Accepted: 22 February 2023

DOI: 10.1002/asna.20230022

Astronomische Nachrichten

ORIGINAL ARTICLE

Optical spectroscopy of Be stars: Peak separation of Balmer emission lines

Radoslav K. Zamanov[1] | **Kiril A. Stoyanov**[1] | **Stefan Y. Stefanov**[1] | **Michael F. Bode**[2,3] | **Milen S. Minev**[1]

[1]Institute of Astronomy and National Astronomical Observatory, Bulgarian Academy of Sciences, Sofia, Bulgaria

[2]Astrophysics Research Institute, Liverpool John Moores University, Liverpool, UK

[3]Office of the Vice Chancellor, Botswana International University of Science and Technology, Palapye, Botswana

Correspondence
Radoslav K. Zamanov, Institute of Astronomy and National Astronomical Observatory, Bulgarian Academy of Sciences, 72 Tsarigradsko Shose, 1784 Sofia, Bulgaria.
Email: rkz@astro.bas.bg

Abstract

The Be stars display variable optical emission lines originating in the circumstellar disc. Here we analyze high resolution spectroscopic observations of Be stars and the distance between the peaks of Hα, Hβ, and Hγ emission lines (ΔV_α,ΔV_β, and ΔV_γ respectively). Combining published data, spectra from the ELODIE archive (obtained in the period 1998–2003) and Rozhen spectra (obtained 2015–2023) of 93 Be stars, we find a set of relations connecting ΔV_α, ΔV_β and ΔV_γ. They are effective for $30 \leq \Delta V_\alpha \leq 500$ km s^{-1}, $80 \leq \Delta V_\beta \leq 600$ km s^{-1}, and $40 \leq \Delta V_\gamma \leq 300$ km s^{-1}. The new equations are in the form $y = ax + b$ and are valid for a wider velocity range than in previous studies.

KEYWORDS

binaries: spectroscopic, stars: emission-line, Be, stars: winds, outflows

1 | INTRODUCTION

The Be stars are fast-rotating B-type stars that, at some point in their lives, have shown spectral lines in emission (Porter & Rivinius, 2003). They are main sequence or evolved stars, belonging to luminosity classes III–V and having masses and radii ranging between M~3.6–20 $M_\odot$ and R~2.7–15 $R_\odot$ (Cox & Pilachowski, 2000). In the optical spectra, the most prominent observational characteristics of Be stars are variable emission lines of different chemical elements such as hydrogen, helium, iron, and so forth. The emission lines may change their intensity and even disappear during the star's life. In addition, an infrared excess is present in their continuum (Gehrz et al., 1974). The emission lines and the infrared excess indicate the presence of a geometrically thin, equatorial, gaseous, decretion disc, which orbits the star in near-Keplerian rotation (Rivinius et al., 2013). Interferometric observations confirm the disc-like structure of the circumstellar material (Cochetti et al., 2019; Meilland et al., 2007). The emission lines can be symmetric or asymmetric, with a double-peak or more complicated structure (Hummel & Vrancken, 1995; Silaj et al., 2010), and the peaks' separation can be used for an estimation of the disc radius and to test theoretical models.

In this note, we analyze the separation of the peaks of the Balmer emission lines formed in the circumstellar disc and the relations between them.

2 | OBSERVATIONS

We analyze 35 optical spectra of Be stars obtained with the ESpeRo Echelle spectrograph (Bonev et al., 2017) on the 2.0 m telescope of the Rozhen National Astronomical Observatory, Bulgaria, and 27 spectra from the ELODIE archive (Ilovaisky et al., 2008), obtained with the 1.93 m telescope of the Observatoire de Haute-Provence, France. Both instruments are fiber-fed Echelle spectrographs providing high resolution spectra in the optical range. The ESpeRo spectrograph has a resolution of ~30,000 and

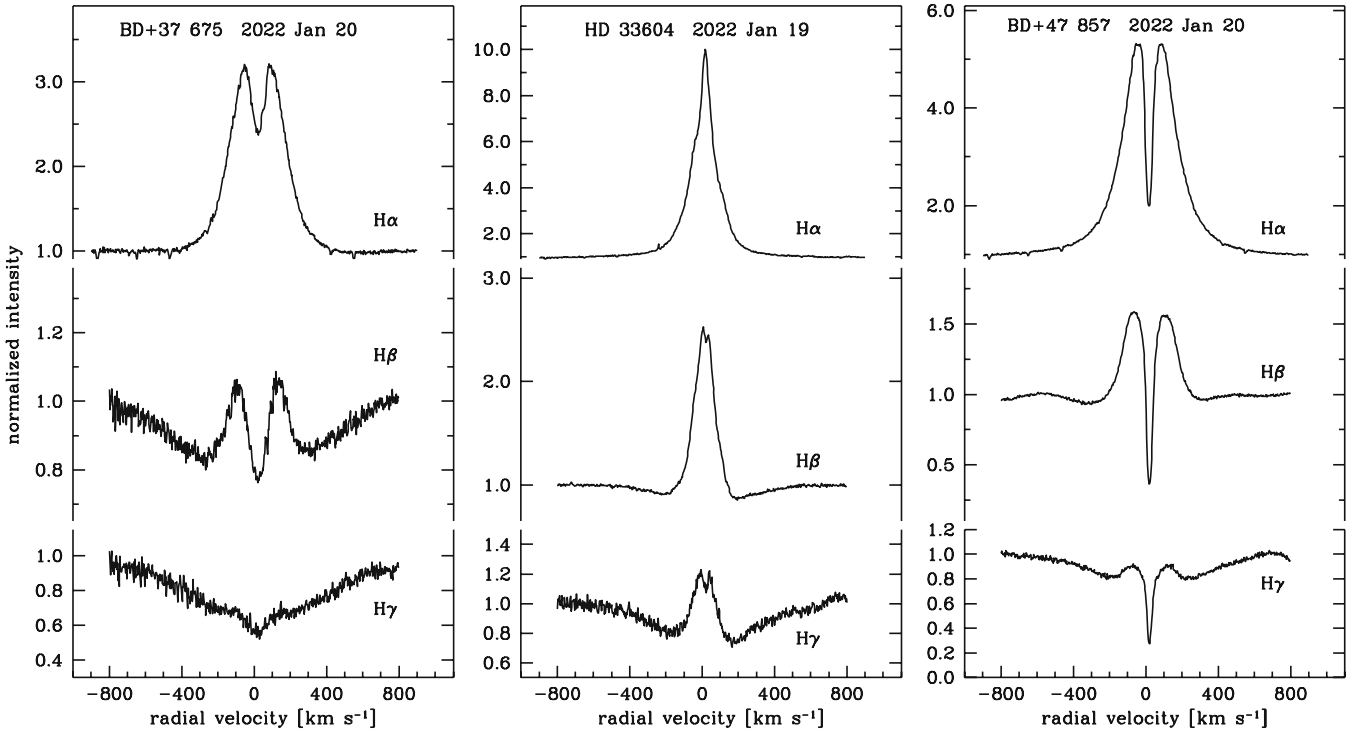

FIGURE 1 Examples of the profiles of Hα, Hβ, and Hγ lines. The object and the date of observation are marked at the top of each panel.

covers the range 3900–9000 Å. The ELODIE spectrograph has a resolution of ∼42,000 and covers the range 3895–6815 Å. The spectra Rozhen spectra were obtained during the period 2015–2023, the ELODIE–1997–2003. Some examples of the profiles of Hα, Hβ, and Hγ emission lines are shown in Figure 1.

On the spectra, we measure the distance between the peaks of the Balmer emission lines Hα (ΔV_α), Hβ (ΔV_β), and Hγ (ΔV_γ). The measurements are listed in Tables 1 and 2. These parameters are identical to $(\Delta\lambda)_s$, as shown on Figure 3 of Slettebak (1976). To measure the position, we applied Gaussian fitting at the top of each peak, as shown in figure 5 in the Appendix. The typical errors are ±5 km s^{-1} for ΔV_α, ±7 km s^{-1} for ΔV_β, and ±10 km s^{-1} for ΔV_γ.

3 | RELATIONS

For the Be stars, Hanuschik et al., (1988) find that the peak separations of Hβ and Hα emission lines follow approximately the relation $\Delta V_\beta \approx 1.8\Delta V_\alpha$. Dachs et al. (1992) find that average $\Delta V_\beta/\Delta V_\alpha = 1.6 - 1.8$. Using more data, we have found that this relation is not valid above $\Delta V_\alpha \approx$ 200 km s^{-1}, and a linear fit of the type $y = a + bx$ is more appropriate. In Figure 2 we plot ΔV_β versus ΔV_α for 56 Be stars. In this figure, the black circles are from Hanuschik et al. (1988), Dachs et al. (1992) and Catanzaro (2013). The green squares are ELODIE spectra (Table 2). The red pluses are Rozhen data. The Rozhen data include the new spectra from Table 1, and the published spectra obtained with the same telescope setup (Zamanov et al., 2016; Zamanov et al., 2022). We find the following relationship between ΔV_α and ΔV_β:

$$\Delta V_\beta = 1.01(\pm0.01)\ \Delta V_\alpha + 64.2(\pm2.5)\,\mathrm{km\,s^{-1}} \quad (1)$$

This relation is valid for the range of ΔV_α from 40 to 530 km s^{-1}. It is very similar to our finding for a smaller sample and smaller range (Zamanov et al., 2022). As expected, there is a very strong correlation between these two quantities, with a Pearson correlation coefficient of 0.95, Spearman's rank correlation of 0.93, and significance 10^{-20}.

In Figure 3, we plot ΔV_γ versus ΔV_β. The black circles are data from Slettebak (1976) and Hanuschik et al. (1988) The green squares are ELODIE data, the red pluses are Rozhen data. For the Be stars, Hanuschik et al. (1988) find that the peak separations of Hβ and Hγ emission lines are connected as $\Delta V_\gamma = 1.2\Delta V_\beta$. Here, using more data, we find the following connection between ΔV_β and ΔV_γ:

$$\Delta V_\gamma = 1.034(\pm0.031)\ \Delta V_\beta + 14.9(\pm4.2)\quad \mathrm{km\ s^{-1}} \quad (2)$$

This relation is valid for the range of ΔV_β from 20 to 340 km s^{-1}. There is a very strong correlation

TABLE 1 Rozhen spectra—ΔV_α, ΔV_β, and ΔV_γ.

Object		File	ΔV_α [km s^{-1}]	ΔV_β [km s^{-1}]	ΔV_γ [km s^{-1}]
BD−00 3543	HD 173371	20220520.01.fit	223.4	278.7	—
BD−00 3543	HD 173371	20220520.02.fit	223.7	281.4	—
BD−00 3543	HD 173371	20220512.1800s.fit	218.2	269.3	—
BD+02 3815	HD 179343	20220512.1800s..fit	227.4	270.7	—
BD+02 3815	HD 179343	20220521.01.fit	230.2	277.1	—
BD+02 3815	HD 179343	20220521.02.fit	229.9	278.3	
BD+05 3704	HD 168797	20220520.01.fit	549.6	651.1	
BD+05 3704	HD 168797	20220520.02.fit	521.1	658.3	
BD+30 0591	X Per	20151223.1.fit	102.9	143.2	168.4
BD+30 0591	X Per	20160130.fit	96.8	127.0	135.7
BD+30 0591	X Per	20161211.fit	59.2	132.7	154.3
BD+30 0591	X Per	20171230.fit	127.0	150.6	163.5
BD+37 0675	HD 18552	20220120.1.120s.fit	151.2	234.2	
BD+37 0675	HD 18552	20220120.1.600s.fit	151.6	228.3	257.9
BD+37 0675	HD 18552	20220120.2.120s.fit	150.2	236.5	
BD+37 0675	HD 18552	20220120.2.600s.fit	150.1	230.9	280.7
BD+47 0857	psi Per	20220120.1.120s.fit	133.4	—	
BD+47 0857	psi Per	20220120.1.300s.fit	132.2	174.0	205.1
BD+47 0857	psi Per	20220120.2.120s.fit	132.9	174.8	201.2
BD+47 0857	psi Per	20220120.2.300s.fit	131.7	176.5	206.9
BD+50 0825	HD 23552	20,220320.1.20min.fit	184.0	261.2	
BD+50 0825	HD 23552	20220320.2.20min.fit	187.0	245.1	
BD+40 1213	HD 33604	20220119.1.20min.fit	—	29.8	39.7
BD+40 1213	HD 33604	20220119.2.20min.fit	—	26.5	48.7
BD+42 1376	HD 37657	20220119.1.20min.fit	412.7	467.4	—
BD+42 1376	HD 37657	20220119.2.20min.fit	404.2	421.1	—
CSI+44-04374	LS V+44 17	20161211.fit	290.6	346.9	—
CSI+44-04374	LS V+44 17	60m.1.20230211.fit	250.8	338.9	—
BD+53 2790	4U 2206+54	20160620.fit	467.0	503.4	—
BD+53 2790	4U 2206+54	20151227.fit	493.1	582.7	—
BD+53 2790	4U 2206+54	20190819.fit	516.4	599.7	—
BD+53 2790	4U 2206+54	20200905.fit	493.0	525.4	—
CSI+59-01302	LS I +59 79	20160621.fit	177.4	265.1	—
CSI+59-01302	LS I +59 79	20160923.fit	179.5	249.5	—
BD+59 0144	gamma Cas	20160621.1.fit	—	138.7	176.2
BD+59 0144	gamma Cas	20160621.2.fit	—	132.0	172.3

TABLE 2 ELODIE spectra—ΔV_α, ΔV_β, and ΔV_γ.

Object		File name	ΔV_α [km s^{-1}]	ΔV_β [km s^{-1}]	ΔV_γ [km s^{-1}]
BD+00 4872	pi Aqr	elodie_20011222_0005.fits	563.8	—	—
BD+04 1002	omega Ori	elodie_19981123_0035.fits	244.1	339.8	370.1
BD+04 1002	omega Ori	elodie_19981125_0014.fits	242.1	346.0	366.9
BD+04 1002	omega Ori	elodie_19981126_0032.fits	242.4	350.6	348.0
BD+04 1002	omega Ori	elodie_19981125_0033.fits	245.2	333.1	340.3
BD+04 3570	66 Oph	elodie_20030808_0013.fits	142.5	211.8	243.9
BD+04 3570	66 Oph	elodie_20030811_0021.fits	140.0	214.3	253.2
BD+04 3570	66 Oph	elodie_20030819_0014.fits	142.2	218.4	234.4
BD+08 1774	beta CMi	elodie_20020328_0018.fits	133.3	215.3	—
BD+11 4784	31 Peg	elodie_20011222_0006.fits	36.7	67.9	92.3
BD+23 0558	28 Tau	elodie_20011121_0042.fits	91.0	150.2	181.4
BD+23 0558	28 Tau	elodie_20011220_0013.fits	98.8	139.0	167.2
BD+23 0558	28 Tau	elodie_20030124_0005.fits	105.7	153.6	189.8
BD+30 0591	X Per	elodie_20041117_0010.fits	110.8	167.4	189.5
BD+34 4371	ups Cyg	elodie_20030809_0026.fits	59.1	106.8	153.7
BD+34 4371	ups Cyg	elodie_20030811_0030.fits	45.1	107.8	148.6
BD+34 4371	ups Cyg	elodie_20030819_0022.fits	56.0	110.8	148.2
BD+47 0857	psi Per	elodie_20030814_0023.fits	126.8	173.1	187.7
BD+47 0857	psi Per	elodie_20030815_0025.fits	134.5	172.7	193.8
BD+47 0857	psi Per	elodie_20030819_0046.fits	134.9	172.9	192.4
BD+49 0444	phi Per	elodie_19970917_0023.fits	194.5	218.7	234.9
BD+49 0444	phi Per	elodie_19970917_0024.fits	189.8	220.8	242.2
BD+64 1527	6 Cep	elodie_20030818_0019.fits	65.4	136.8	177.3
BD+64 1527	6 Cep	elodie_20030819_0017.fits	65.6	132.3	172.7
BD+64 1527	6 Cep	elodie_20030819_0025.fits	66.0	133.2	174.0
BD+70 0703	kappa Dra	elodie_20000126_0038.fits	116.5	198.1	212.2
BD+70 0703	kappa Dra	elodie_20000128_0020.fits	100.7	200.0	216.3

between these two quantities, with a Pearson correlation coefficient 0.97, Spearman's rank correlation 0.96, and significance 10^{-18}.

For 14 objects, we have ΔV_γ and ΔV_α on the same spectrum, a total of 36 data points, because some objects are observed several times. In Figure 4 we plot ΔV_γ versus ΔV_α. These data points refer to spectra on which both ΔV_α and ΔV_γ can be measured. We are not able to measure ΔV_α and ΔV_γ on each spectrum because: (1) if the Hα emission is strong, the Hα peaks are very close to one another and can merge; (2) if the Hα emission is weak, the emission peaks in Hγ are not visible; and (3) the sensitivity of the ESpeRo spectrograph is lower at Hγ. From Equations (1) and (2), we expect the following connection between ΔV_γ and ΔV_α:

$$\Delta V_\gamma = 1.04\ \Delta V_\alpha + 81.8 \quad \text{km s}^{-1} \tag{3}$$

This equation is represented as a blue dashed line in Figure 4.

Because there are some objects with one measurement and a few objects with three to four measurements, we performed the linear fit using different subsamples (bootstrap technique, e.g. Efron (1979)) in a way to have in the subsamples one or two measurements for each object and thus not to give too much weight to the objects with four

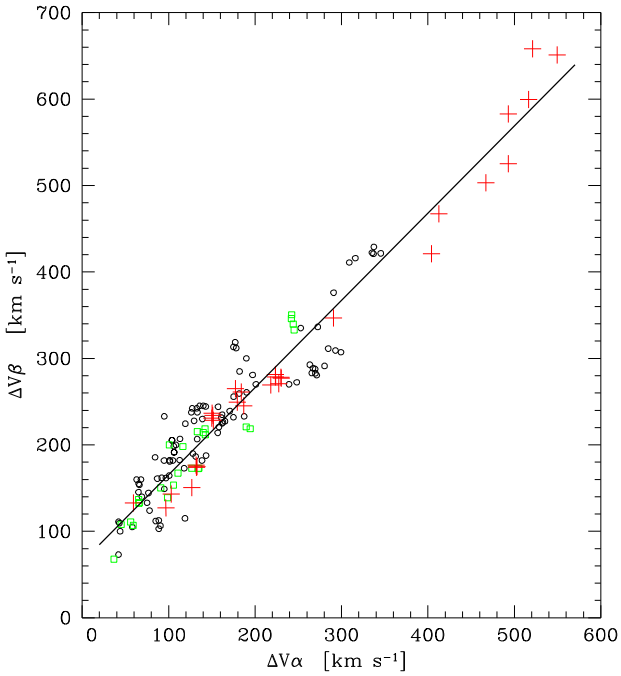

FIGURE 2 ΔV_β versus ΔV_α for Be stars. The black circles are data from the literature, the green squares are ELODIE data, the red pluses are Rozhen data. The solid line is the linear fit $\Delta V_\beta = 1.01\Delta V_\alpha + 64.2$ km s^{-1}.

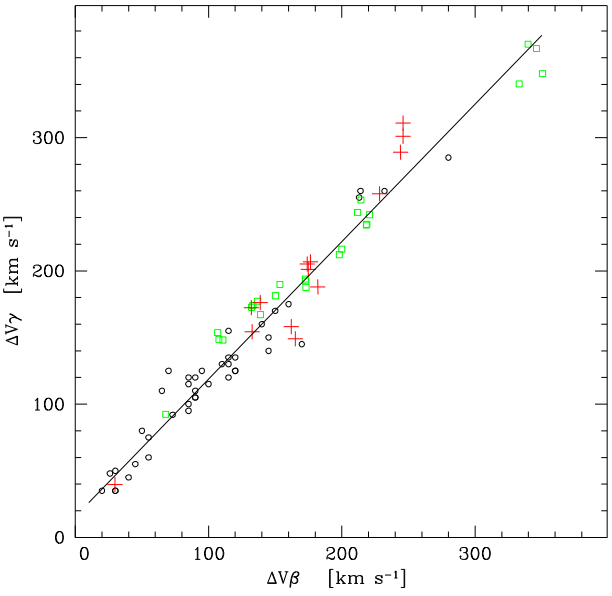

FIGURE 3 ΔV_γ versus ΔV_β for Be stars. The symbols are as in Figure 2. The black solid line is the linear fit $\Delta V_\gamma = 1.03\Delta V_\beta + 15.7$ km s^{-1}.

measurements. A linear fit in the form $y = ax + b$ gives coefficients in the range $0.98 < a < 1.11$ and $71.3 \leq b \leq 82.6$, with average values $a = 1.065$ and $b = 74.8$:

$$\Delta V_\gamma = 1.065(\pm 0.062)\ \Delta V_\alpha + 74.8(\pm 6.2) \quad \text{km s}^{-1} \qquad (4)$$

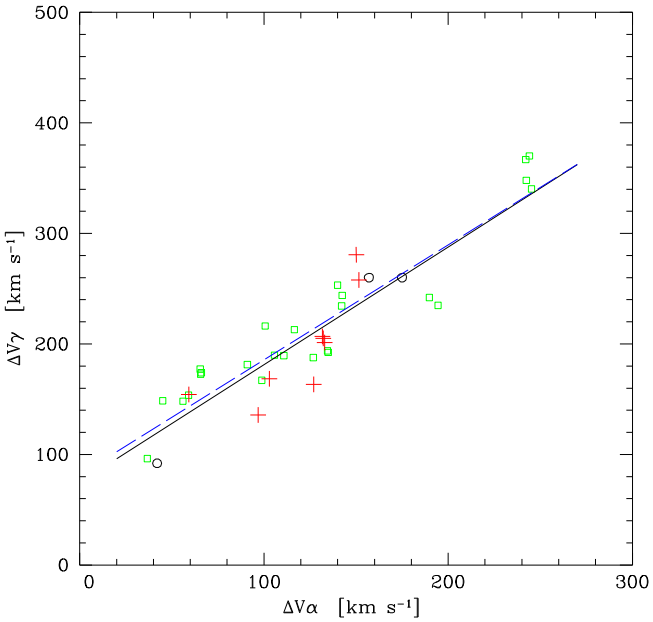

FIGURE 4 ΔV_γ versus ΔV_β for Be stars. The symbols are the same as in Figure 2, and represent the spectra on which both ΔV_γ and ΔV_α are measured simultaneously. The blue dashed line is Equation (3), and the black solid line is the fit as given by Equation (4).

This fit is represented as a black solid line in Figure 4. The correlation is strong, with a Pearson correlation coefficient of 0.90, Spearman's rank correlation 0.91, and significance 10^{-9}.

The black solid line (derived from the fit over the data) and the blue dashed line (based on the relationships ΔV_α vs. ΔV_β and ΔV_β vs. ΔV_γ) are similar, which confirms that the results are self-consistent. In all three cases (ΔV_β vs. ΔV_α, ΔV_γ vs. ΔV_β, and ΔV_γ vs. ΔV_α, presented in Figures 2, 3, and 4, respectively), we find a linear relationship of the type $y = ax + b$, with $a \approx 1.0$.

4 | DISC SIZE

In the Be stars, the distance between the peaks of the Hα emission line can be regarded as a measure of the outer radius (R_{disc}) of the emitting disc (e.g., Huang (1972)).

$$R_{disc} = R_1 \left(\frac{2\ v \sin i}{(1-\epsilon)\ \Delta V\alpha} \right)^2, \qquad (5)$$

where G is the gravitational constant, M_1 is the mass of the Be star, $v \sin i$ is the projected rotational velocity, $\sin i$ is the inclination to the line of sight. The term $(1 - \epsilon)$ represents the fact that the Be stars are rotating below the critical value (Porter & Rivinius, 2003).

The relations between ΔV_γ, ΔV_β, and ΔV_α give us the possibility to estimate $R_{\rm disc}$, when two peaks are visible in Hβ,

$$R_{\rm disc} = R_1 \left(\frac{1.01^*2 \ v \sin i}{(1-\epsilon) \ \left(\Delta V_\beta - 64.2\right)} \right)^2, \qquad (6)$$

or in Hγ emission:

$$R_{\rm disc} = R_1 \left(\frac{1.065^*2 \ v \sin i}{(1-\epsilon) \ \left(\Delta V_\gamma - 74.8\right)} \right)^2, \qquad (7)$$

where ΔV_β, ΔV_γ, and $v \sin i$ are in km s^{-1}.

Radius estimation through the method of Huang (1972) is a good approximation for symmetric profiles with a double peaked Hα. If the two peaks of Hα are not clearly visible, the equivalent width of Hα emission can be used instead (e.g., section 3 of Coe et al. (2006), and equation (5) in Zamanov et al. (2022)). The relationships given above by Equations (6) and (7) offer a third possibility.

5 | DISCUSSION

Recently, Wang et al. (2018) and Wang et al. (2021) using the ultraviolet (UV) spectra from hubble space telescope (HST) and ultraviolet explorer (IUE), searched and found hot subdwarf companions of Be stars. Their results indicate that probably the rapid rotation of most Be stars is a result of mass transfer in a close binary system, as suggested by Pols et al. (1991). In this scenario, many Be stars are expected to have companions that are the remnants of the mass donor. The donor star might be stripped and become a hot subdwarf star in a Be+sdO binary, it might explode to create a neutron star or black hole in a Be/x-ray binary, or the binary might be disrupted by the supernova explosion (Postnov & Yungelson, 2014).

Potentially, the deviations of individual objects from the average behavior (as expressed in Equations (1), (2), and (4)) can be used to investigate the influence of the secondary on the Be disc structure, disc truncation, (because the truncation occurs only at certain radii; Okazaki & Negueruela (2001)), warping of the disc (Martin et al., 2011), and so forth. The correlations can also be useful to test the theoretical models for formation of the emission lines in Be discs like those presented in figure 14 of Iwamatsu & Hirata (2008).

The Be stars show spectral variability both on short time-scales—hours to months (Paul et al., 2017; Porter & Rivinius, 2003) and long time-scales—up to years and decades (Mennickent et al., 1994). One major observational aspect of Be stars is that some of them change phase from Be − Be-shell − normal B star − Be. It will be interesting to follow the evolution of Be stars on these diagrams during the phase changes.

6 | CONCLUSIONS

We analyzed high resolution spectra of Be stars. We find the relationships between separations of the peaks of the Hα, Hβ, and Hγ emission lines. The correlations found should be useful for future theoretical modeling and a better understanding of the circumstellar discs of the Be stars in general.

ACKNOWLEDGMENTS

This work was supported by the Bulgarian National Science Fund project KP-06-H28/2 08.12.2018 "Binary stars with compact object."

FUNDING INFORMATION

Bulgarian National Science Fund, project KP-06-H28/2 08.12.2018 "Binary stars with compact object".

CONFLICT OF INTEREST

The authors declare no potential conflict of interests.

ORCID

Radoslav K. Zamanov https://orcid.org/0000-0003-0973-3764

Kiril A. Stoyanov https://orcid.org/0000-0002-6149-9111

REFERENCES

Bonev, T., Markov, H., Tomov, T., et al. 2017, *Bulg. Astron. J.*, *26*, 67.

Catanzaro, G. 2013, *A & A*, *550*, A79.

Cochetti, Y. R., Arcos, C., Kanaan, S., Meilland, A., Cidale, L. S., & Curé, M. 2019, *A & A*, *621*, A123.

Coe, M. J., Reig, P., McBride, V. A., Galache, J. L., & Fabregat, J. 2006, *MNRAS*, *368*(1), 447.

Cox, A. N., & Pilachowski, C. A. 2000, *Phys. Today*, *53*(10), 77.

Dachs, J., Hummel, W., & Hanuschik, R. W. 1992, *A & AS*, *95*, 437.

Efron, B. 1979, *Ann. Stat.*, *7*, 1.

Gehrz, R. D., Hackwell, J. A., & Jones, T. W. 1974, *ApJ*, *191*, 675.

Hanuschik, R. W., Kozok, J. R., & Kaiser, D. 1988, *A & A*, *189*, 147.

Huang, S.-S. 1972, *ApJ*, *171*, 549.

Hummel, W., & Vrancken, M. 1995, *A & A*, *302*, 751.

Ilovaisky, S., Prugniel, P., Soubiran, C., Koleva, M., & Le Coroller, H. 2008, in: *Astronomical Spectroscopy and Virtual Observatory*, eds. European Space Agency (Paris), M. Guainazzi & P. Osuna, 47.

Iwamatsu, H., & Hirata, R. 2008, *PASJ*, *60*, 749.

Martin, R. G., Pringle, J. E., Tout, C. A., & Lubow, S. H. 2011, *MNRAS*, *416*(4), 2827.

Meilland, A., Stee, P., Vannier, M., et al. 2007, *A & A*, *464*(1), 59.

Mennickent, R. E., Vogt, N., & Sterken, C. 1994, *A & AS*, *108*, 237.

Okazaki, A. T., & Negueruela, I. 2001, *A & A*, *377*, 161.
Paul, K. T., Shruthi, S. B., & Subramaniam, A. 2017, *J. Astrophys. Astron.*, *38*(1), 6.
Pols, O. R., Cote, J., Waters, L. B. F. M., & Heise, J. 1991, *A & A*, *241*, 419.
Porter, J. M. & Rivinius, T., 2003, *PASP*, *115*(812), 1153.
Postnov, K. A., & Yungelson, L. R. 2014, *Liv. Rev. Relat.*, *17*(1), 3.
Rivinius, T., Carciofi, A. C., & Martayan, C. 2013, *A &A Rev.*, *21*, 69.
Silaj, J., Jones, C. E., Tycner, C., Sigut, T. A. A., & Smith, A. D. 2010, *ApJS*, *187*(1), 228.
Slettebak, A. 1976, in: *Be and Shell Stars, Vol. 70*, Reidel Pub. Co. (Dordrecht), ed. A. Slettebak, 123.
Wang, L., Gies, D. R., & Peters, G. J. 2018, *ApJ*, *853*(2), 156.
Wang, L., Gies, D. R., Peters, G. J., Götberg, Y., Chojnowski, S. D., Lester, K. V., & Howell, S. B. 2021, *AJ*, *161*(5), 248.
Zamanov, R. K., Stoyanov, K. A., Marchev, D., et al. 2022, *Astron. Nachr.*, *343*, e24019.
Zamanov, R. K., Stoyanov, K. A., Martí, J., Latev, G. Y., Nikolov, Y. M., Bode, M. F., & Luque-Escamilla, P. L. 2016, *A & A*, *593*, A97.

AUTHOR BIOGRAPHY

Radoslav K. Zamanov: MSc - Sofia University "Saint Kl. Ohridski" (1989); PhD - National Astronomical Observatory Rozhen, Bulgarian Academy of Sciences (1997); fellow - Universidad de Jaen, Spain (2000); postdoc - Osservatorio Astronomico di Padova, Padova, Italy (2001–2003); postdoc research assistant - Astrophysics Research Institute, Liverpool John Moores University, UK (2003–2005); senior researcher (2005–2012), professor of astrophysics and stellar astronomy (since 2012) - Institute of Astronomy and NAO, Bulgarian Academy of Sciences.

SUPPORTING INFORMATION

Additional supporting information can be found online in the Supporting Information section at the end of this article.

How to cite this article: Zamanov, R. K., Stoyanov, K. A., Stefanov, S. Y., Bode, M. F., & Minev, M. S. 2023, *Astron. Nachr.*, e20230022. https://doi.org/10.1002/asna.20230022